Effects of model inaccuracies in Model Predictive Filtering MRTI

Henrik Odéen[1,2], Nick Todd[1], Chris Dillon[3], Allison Payne[1], and Dennis L Parker[1]

[1]*Utah Center for Advanced Imaging Research, Department of Radiology, University of Utah, Salt Lake City, Utah, United States,* [2]*Department of Physics and Astronomy, University of Utah, Salt Lake City, Utah, United States,* [3]*Department of Bioengineering, University of Utah, Salt Lake City, Utah, United States*

Introduction

One of the main challenges in MR guided thermal therapies is achieving sufficiently fast temperature measurements over a large enough field-of-view (FOV) to adequately monitor heat deposition. One popular approach to achieve faster imaging is k-space subsampling, which for MR temperature imaging (MRTI) has been combined with constrained [1,2] and model based [3-5] reconstruction approaches. This work investigates how model parameter inaccuracies, k-space reduction factor (*R*), and rate of temperature rise affect the accuracy of MRTI when using the Model Predictive Filtering (MPF) [3] approach.

$$\rho C \frac{\delta T}{\delta t} = k\nabla^2 T - WC(T - T_{blood}) + Q \quad \textbf{(1)}$$

$$\phi_{n+1} = \phi_n + \gamma B_0 \alpha TE(T_{n+1} - T_n) \quad \textbf{(2)}$$

Equation 1. PBTE: ρ=density, C=specific heat, T=temperature, k=thermal conductivity, W=perfusion parameter, and Q=power density. **Equation 2.** PRF shift: ϕ=phase, Υ=gyromagnetic ratio, B_0=field strength, α=PRF coefficient, TE=echo time.

Methods

MPF Temperature maps for time-frame (n+1) are calculated by combining subsampled k-space data with a forward-prediction of the temperature from time-frame (n) using a thermal model (Pennes Bioheat Transfer equation (PBTE), equation 1). *k* and *Q* are obtained from low-power heatings using recently published methods [6,7], and tabular values are used for ρ (1000 kg /m^3) and *C* (2760 J/kg/°C). After combination and projection into image space, temperatures are calculated from the image phase with the proton resonance frequency (PRF) shift method, equation 2.

Simulations 4 types of simulations were performed for 3 heating durations (21/42/63s) and 2 US power levels (corresponding to 9°C/18°C heatings). Lower power heatings were used for thermal property determination (*k*/*Q*), and higher power heatings were used for Model/MPF accuracy evaluation. The high power heatings for the three durations correspond to temperature rise rates of 0.86/0.43/0.30 °C/s, respectively.

1. Model-only accuracy To assess how errors in thermal properties (*k*/*Q*) affect temperature predictions when using only the thermal model. High power heatings were simulated with PBTE with errors in *k* and *Q* ranging from -50% to +50%, and compared to "truth" simulated without errors.

2. Model-only predictive capability To assess how well thermal properties determined from a low power heating can be used to forward predict a high power heating. Estimates of *k* and *Q* from a low power heating (created with random zero-mean Gaussian noise, with standard deviation (std) corresponding to 0.20°C) were used to simulate a high power heating with PBTE, and then compared to "true" high power heating. This was repeated 25 times each for the 3 durations, each time with a new set of noise.

3. MPF Robustness To assess how errors in thermal properties affect temperature predictions from the MPF algorithm. Same as *Model only accuracy* but simulated subsampled k-space (with *R*=4/6/12) and the MPF algorithm was used.

4. MPF Accuracy To assess how well thermal properties from a low power heating used in combination with subsampled k-space (with noise added as described above) in the MPF algorithm can estimate temperatures. Same as *Model-only predictive capabilities* but subsampled k-space (with *R*=4/6/12) and the MPF algorithm was used. Repeated 25 times each for the 3 durations and 3 *R*'s, each time with a new set of noise.

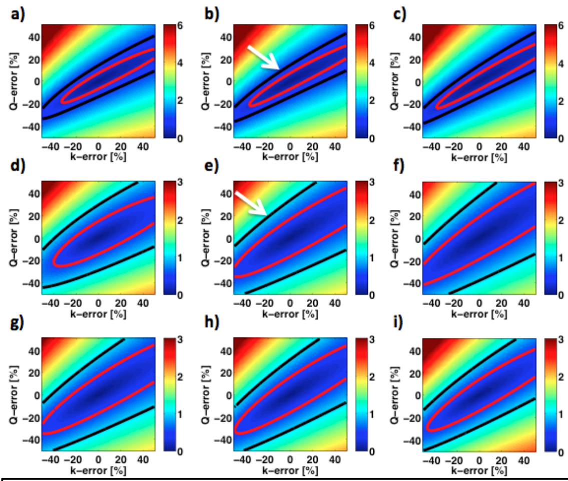

Figure 1. RMSE for a) – c) *Model only accuracy* for 21s, 42s, and 63s heatings, respectively, and d) – f) corresponding results for *MPF Robustness* with R=4. g) – h) *MPF Robustness* for 42s and R=4, 6, and 12, respectively. Black/red contour represents RMSE of 1°C/0.5°C.

Ex-vivo experiments 5 sets of HIFU experiments, where each set consisted of 3 heatings: #1 Low power and small FOV (for thermal properties determination), #2 High power and small FOV (used as "truth"), and #3 High power and large FOV (subsampled with *R*=4/6/12), were performed in 3 tissue samples of porcine muscle, for a total of 15 sets and 45 heatings. Heatings were performed at 14/28W (low/high power) for 21s, 14/28W for 42s, and 12/24W for 63s, in the three tissue samples, respectively. All heatings were performed with a phased array transducer (256 elements, 1 MHz, Imasonic, Besançon, France) and all MR imaging was performed with a 3D GRE segmented EPI pulse sequence on a 3T MRI scanner (TIM Trio, Siemens Medical Solutions, Erlangen, Germany). Imaging parameters included 1.5x1.5x2.0 mm voxels (zero-filled to 0.5 mm isotropic), 12/48 slices (small/large FOV), TR/TE=36/11ms, BW=752Hz/px, ETL=9. Acquisition time was 5.20s for heatings #1 and #2, and 5.20/3.46/1.73s for #3 with R=4/6/12, respectively. Temperature rises were calculated with the PRF shift method, equation 2. Subsampling was done in the ky (phase encode) direction, while fully sampling the kx and kz (read out/slice encode) directions. Errors for both simulations and experiments were evaluated as the root-mean-square-error (RMSE) of all voxels that had temperatures >30% of the hottest voxel in respective "truth".

Results and Conclusions

Simulations Figure 1 shows *Model-only accuracy* and *MPF Robustness* results for three durations and three *R's*. Comparing a) - c) to d) – f) it can be seen that for all durations the RMSE for MPF is substantially smaller than for Model-only. White arrows in b) and e) e.g. show that errors in *k*/*Q* of -9%/+9% result in a RMSE of 1°C for *Model-only*, while for *MPF* errors of -17%/+21% result in a 1°C RMSE. Figure 2 shows RMSEs for *Model only prediction* and *MPF Accuracy* simulations (in blue). From the total of 300 low power heatings in the *Model-only predictive* and *MPF Accuracy* simulations *k* and *Q* as estimated using [6,7] were slightly over-estimated, 103±0.9% and 102±2.5%, respectively, compared to "true" values.

Ex-vivo experiments Mean and std of the temperature rise in the hottest voxel in the 5 *ex-vivo* "truth" heatings (#2 above) for each duration were 15.8±0.98°C, 19.3±0.37°C, and 17.3±0.89°C, corresponding to 0.75, 0.46, and 0.28°C/s. *Ex-vivo Model-only prediction* and *MPF Accuracy* results are shown in figure 2 (in red). The mean and std of the thermal conductivity (*k*) from the 15 low power heatings (#1 above) in the 3 samples were 0.41±0.03 W/m/°C. The *ex-vivo* data for all three durations and *R*'s were also reconstructed using this mean value of *k*, to investigate the possibility of using a "tabular" value for *k* (green in figure 2b).

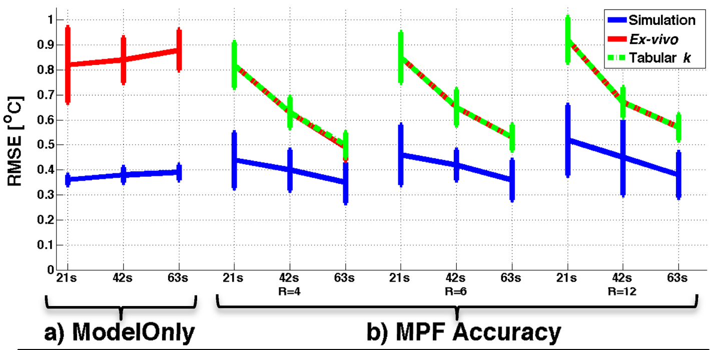

Figure 2. Mean and std of RMSE for a) *Model only* experiment, and b) *MPF accuracy* experiment, for all durations and *R*'s.

From figure 2a) it can be seen that when only the model is used errors in the thermal properties have a greater impact the longer the heating, and RMSE increases slightly with heating duration for both simulations and experiments. Figure 2b) shows that for MPF there is a decrease in RMSE for longer heating durations (slower heatings), while for a given duration the RMSE increases for higher R, this is also seen in figure 1 d)-f) and g)-i), respectively. Comparing using individual/mean values of *k* (red/green in figure 2b) it can be seen that using a "tabular" value does not increase errors. In summary, the current work shows that the accuracy of temperature measurements is increased when using MPF compared to model only, RMSE decrease with slower heatings (for MPF), and increase with higher R. No increase in error was observed when using a "tabular" value for *k*.

References [1] Todd *et al.* MRM 2009. [2] Gaur and Grissom. ISMRM 2013. [3] Todd *et al.* MRM 2010. [4]. Roujol *et al.* IEEE Trans. Med. Imag. 2012. [5] Fuentes IEEE Trans. Med. Imag. 2012. [6] Dillon *et al.* Phys Med Biol 2012. [7] Dillon *et al.* ISMRM 2013. **Acknowledgements** This work was supported by The Focused Ultrasound Surgery Foundation, Siemens Healthcare, The Ben B. and Iris M. Margolis Foundation, and NIH grants F32 EB012917-02, and R01s EB013433, and CA134599.